

## HYDRODYNAMIC CHARACTERIZATION IN A RACEWAY BIOREACTOR WITH DIFFERENT STIRRERS

## CARACTERIZACIÓN HIDRODINÁMICA DE UN BIORREACTOR RACEWAY CON DIFERENTES AGITADORES

S.S. Bautista-Monroy<sup>1</sup>, J.C. Salgado-Ramírez<sup>2</sup>, A. Téllez-Jurado<sup>1</sup>, M.R. Ramírez-Vargas<sup>1</sup>, C.A. Gómez-Aldapa<sup>3</sup>, K.J. Pérez-Viveros<sup>1</sup>, S.A. Medina-Moreno<sup>1</sup>, A. Cadena-Ramírez<sup>1\*</sup>

<sup>1</sup>Posgrado en Biotecnología; <sup>2</sup>Programa de Ingeniería Biomédica; Universidad Politécnica de Pachuca, Carretera Pachuca-Cd. Sahagún, km 20, Ex-Hacienda de Santa Bárbara, C.P. 43830, Zempoala, Hidalgo, México. <sup>3</sup>Universidad Autónoma del Estado de Hidalgo, Área Académica de Química, Instituto de Ciencias Básicas e Ingeniería, Ciudad del Conocimiento, Carretera Pachuca-Tulancingo, km 4.5, Col. Carboneras, C.P. 42184, Mineral de la Reforma, Hidalgo, México.

Received: Junio 21, 2018; Accepted: July 26, 2018

### Abstract

Microalgae and cyanobacteria are of great interest for various industries due to the products that can be obtained from them. This makes the study of the cultivation systems of these microorganisms increasing. Such is the case of Raceway bioreactors, which have been analyzed by simulations to study mixing and agitation. Mixing is the most important factor in the growth of photosynthetic microorganisms. In the present work, experimental evidence of hydrodynamic parameters such as;  $Re$ ,  $Fr$ ,  $N_Q$ ,  $N_P$  and  $E_P$  are obtained and flow paths were also obtained within a Raceway bioreactor. It was found that the turbine agitator generated more turbulence, with maximum  $Re$  of 68,959, therefore it is more efficient than the flat paddle agitator, with which a maximum  $Re$  of 57,744 was generated.

**Keywords:** Raceway bioreactor, hydrodynamic, velocimetry by image capture, Reynolds number.

### Resumen

Las microalgas y cianobacterias son de gran interés para diversas industrias debido a los productos que se pueden obtener de ellas. Esto hace que el estudio de los sistemas de cultivo de dichos microorganismos vaya en aumento. Tal es el caso de los biorreactores Raceway, los cuales se han analizado mediante simulaciones para estudiar el mezclado y la agitación. El mezclado es el factor más importante en el crecimiento de los microorganismos fotosintéticos. En el presente trabajo se muestra evidencia experimental de parámetros hidrodinámicos tales como;  $Re$ ,  $Fr$ ,  $N_Q$ ,  $N_P$  y  $E_P$  y además se obtuvieron trayectorias de flujo dentro de un biorreactor Raceway. Se encontró que el agitador de turbina generó más turbulencia, con  $Re$  máximo de 68,959, por lo tanto es más eficiente que el agitador de paletas planas, con el cual se generó un  $Re$  máximo de 57,744.

**Palabras clave:** biorreactor raceway, hidrodinámica, velocimetría por captura de imágenes, número de Reynolds.

## 1 Introduction

There is a great diversity of photosynthetic microorganisms from which value-added products can be obtained (Kanhaiya *et al.*, 2015), among them it is found cyanobacteria and microalgae (Sanjeev Mishra & Kaustubha, 2015; Navarro-Peraza *et al.*, 2017; Martínez-Palma *et al.*, 2015). The massive cultivation of these microorganisms requires adequate exposure to sunlight, as it is their main source of energy (Tomaselli, 2004). Also needs the agitation necessary for all cells to have a good distribution in the

culture and they does not present stratifications in pH, temperature and nutrient concentration (Chisti, 2016). The main systems of cultivation at the industrial level is open systems (Mendoza Guzmán, 2011), which can be natural as rivers and lakes (Richmond, 2004), or, manipulated systems to increase the production of biomass (Borowitzka, 2005), where the bioreactors Raceway can be found (Robles-Heredia *et al.*, 2016). Raceway bioreactor is a rectangular pond with semicircular heads, which has a central barrier to separate it into two channels, it maintains a depth between 15 and 30 cm (Chisti, 2013), and the liquid medium is moved by a paddlewheel (Hazlebeck, 2011).

\* Corresponding author. E-mail: arturocadena@upp.edu.mx

<https://doi.org/10.24275/uam/izt/dcbi/revmexingquim/2019v18n2/Bautista>

issn-e: 2395-8472

This system has the advantage of high durability due to construction materials (Hernández Pérez and Labbé, 2014). Due its geometric simplicity, it is easy to operate, construct and clean, so operating costs are low and it maintains a large cultivation area. The Raceway system must maintain a turbulent flow to ensure sufficient mixing throughout the bioreactor, since agitation is a major factor in the growth of photosynthetic microorganism (Kanhaiya *et al.*, 2015).

A proper agitation keeps the culture in motion and this favors the use of sunlight, increasing the light/dark cycles (Contreras Flores *et al.*, 2003). The agitation decreases the self-shading caused by the same cells on the culture and uniformly distributes nutrients increasing biomass production (Hadiyanto *et al.*, 2013). The mixing is directly related to the Reynolds number ( $N_{Re}$ ). In open channels, the flow is: laminar if  $N_{Re} < 500$ , turbulent if  $N_{Re} > 2,000$  and between both values is transition flow (Mott, 2006), however in Raceway ponds a turbulent flow is considered when Reynolds values higher than 8,000 are reached (Chisti, 2016). However sometimes the channel flow can be laminar with Reynolds values higher than 10,000 (Giles *et al.*, 2003). Maintaining velocity in a range of 0.2 m/s to 0.6 m/s is sufficient to ensure turbulence (Belay, 2002). When the fluid velocity is below to 0.05 m/s, dead zones are found inside the bioreactor (Zeng *et al.*, 2015).

In order to know the hydrodynamic behavior of the Raceway bioreactors, the Reynolds number is generally used (Hadiyanto *et al.*, 2013), but there are other useful parameters for the characterization of the fluid dynamics. It can be mentioned the Froude Number ( $Fr$ ) which represents the type of flow presented into the channel, when  $Fr < 1$  the flow is subcritical or slow,  $Fr=1$  is a critical flow or normal and when  $Fr > 1$  is supercritical or fast (Mott, 2006).

The Power Number ( $N_P$ ) (Li *et al.*, 2014), which is directly related to the energy required to move the paddlewheel; the flow number ( $N_Q$ ) or pumping capacity also relates to the stirrer and hydraulic efficiency (McCabe *et al.*, 2005; Uribe Ramírez *et al.*, 2012). The determination of velocity profiles and dead zones localization is also a important part in the Raceway ponds characterization. However, the type of experimentation is expensive and need time inversion (Ali *et al.*, 2015). Due this, many techniques has been developed, wich includes simulation techniques and mathematic models, like Computational Fluid Dynamics (CFD). CFD can determine the particles behaviour in a liquid phase to obtain velocity field in dinamics systems (Raffo-Durán *et al.*, 2014; Prussi

*et al.*, 2014). Another way to determine the fluid velocity and the Reynolds values is the Particle Images Velocimetry technique (Ronald, 2005), this consist to track a solids tracers movement scattered in a liquid medium (Martinez-Ramírez & Gonzáles, 2006), where images of high, half or low particles density are used to determine the fluid velocity (Martínez Gonzáles, 2014).

The mixing degree in bioreactors depends of the geometry of the vessel and the type of stirrer that is used. Specially, mixing will depend of the geometric relations between stirrer and the vessel. In the case of Raceway pond, it has been reported that the hydrodynamics of the fluid is affected by: stirring velocity, the characteristics of the fluid, geometric characteristics such curves, aspect ratio (channel width/depth) and baffles (Sompech *et al.*, 2012; Ali *et al.*, 2015).

However, until now the stirrer's geometry has not been considered in studies where full mixing is sought. For example, (Li *et al.*, 2014) studied three agitators (zigzagged, curved forward and curved back) but they focus only in turbulent kinetic energy. (Zeng *et al.*, 2015) studied a paddlewheel at different degrees of inclination, however they focus on biomass production but not on hydrodynamics. Additionally, in previous research (Sompech *et al.*, 2012; Prussi *et al.*, 2014) only computational tools and numerical techniques have been used to determine the hydrodynamic parameters, without considering the geometry of the agitator in the behavior of the fluid and in most cases they do not report a turbulent regime.

The aim of the present work is to know the hydrodynamics parameters presents in Raceway bioreactor, using five different geometry stirrers, determining flow patterns by mean trajectories of particles into the fluid. All this with the purpose of reaching mixing profiles with Reynolds values higher than 10,000, determining the relationship between the type of agitator, the flow produced and the geometric relationships of the bioreactor. Raceway pond mixing was studied using a variant of the Particle Images Velocimetry and low density images analysis. By binarized images comparing, the velocity of a particle within the liquid medium was determined. For the hydrodynamic characterization, stirrers geometry were used and compared with the performance of the conventional flat paddles stirrer. All with the ultimate goal of finding the best mixing conditions.

## 2 Materials and methods

### 2.1 Experimental conditions

In this study, a Raceway bioreactor (Figure 1A) was used with the following dimensions; 70 cm long, 50 cm straight zone, 20 cm width, 10 cm channel width and 8 cm depth (Radmann, 2007), in which the behavior of the fluid in motion was analyzed.

Five types of stirrers were used (Figure 1B): turbine type with six curved blades, anchor type paddle, mesh type paddle, double paddle, each one of six blades (McCabe *et al.*, 2005; Geankoplis, 1998) and the classic paddlewheel of 8 flat blades (Chisti, 2016). Characteristics of the stirrers can be observed in the Table 1, and the turn direction is clockwise. Literature mentions the agitator of 4-8 flat blades is commonly used, since that with more than 8 blades the agitator efficiency increase is not significant, however, the increment in the power consumption is high (Borowitzka, 2005; Chisti, 2013). Due this, it was decided to work with 6 blades agitators and compare them with the 8 blades paddlewheel. In addition, three of the agitators (turbine, mesh y double) are designed in such a way that they cover 80% of the diameter and depth of the channel and the anchor stirrer covers a 98% these geometrical characteristics, in order to have the largest contact surface between stirrer blades and water. The stirring motor was a bipolar step motor (Nema 2 V, torque of 4 kg-cm) controlled with an Arduino board. Three angular velocities were tested (20 rpm, 25 rpm and 30 rpm). Since (Ali et al 2014) suggests that the agitation speed must be greater than 20 rpm to have an effective mixing.

To determine the velocity within the biorreactor and trace the flow lines, hydrated hydrogel microspheres with fluorescein were used as a solid tracer, which present two main characteristics; buoyancy and visibility (Martinez-Ramírez & González, 2006), with a diameter of 100  $\mu\text{m}$ . (López Hinojosa, 2006) recommended not to exceed a

particle size of 500  $\mu\text{m}$  so that the particles can be dragged by the flow currents. The density should not be greater than the medium that contains them (Martínez González, 2014), so that average densities of 654  $\text{Kg}/\text{m}^3$  were used, which is similar to cellular density of some cyanobacteria, in this case *Arthrospira maxima*. Water as liquid phase, with density of 1000  $\text{Kg}/\text{m}^3$  and viscosity of 1 cp. The particles were dispersed in the liquid phase, which was illuminated with an ultraviolet light (UVP of 6 W and 365 nm wavelength) inside a dark room, this type of lighting was used to have a controlled light environment, removing the natural light effects and visualize the fluorescent particles. Three videos were taken for each agitation speed, 10 minutes each, with Sunco camera (12 megapixels resolution) configured to take 30 frames per second (fps) placed at a distance of 0.515 m from the bottom of the bioreactor to the camera lens. This was done in order to determine if the trajectories of the particles within the liquid medium have a similar behavior and in this way determine the patterns of the trajectories.

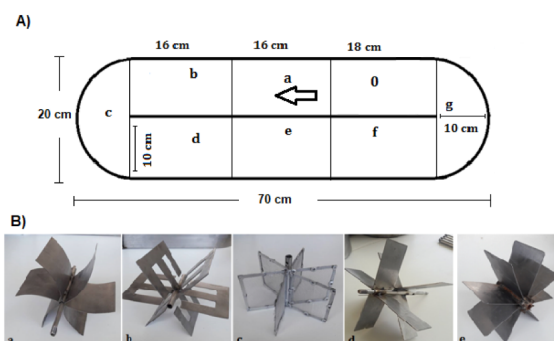


Fig. 1. A). General representation of the Raceway pond and sections: letters a, b, d, e and f correspond to the straight areas of the channels, while c and g represent the first and second curves respectively. 0 zone indicates the stirrer. B) Stirrers applied in the Raceway pond: (a) six blade curved turbine, (b) paddle stirrer type anchor, (c) paddle stirrer type mesh, (d) double blade stirrer and (e) conventional paddlewheel.

Table 1. Characteristics of the stirrers.

Geometry	Double blade	Mesh	Anchor	Turbine	Paddlewheel
Leng (cm)	17.4	17	17	17	17.5
Diameter (cm)	9.8	8	8	8	8
Weight (Kg)	0.285	0.165	0.305	0.33	0.31

## 2.2 Trajectory determination and velocimetry by particles tracking

The determination of trajectories was performed by video analysis and image comparison, using the PROCESSING 3 programming language. Figure 2, describes the proposed methodology for obtaining videos, images Processing and line generation, that correspond to the trajectories. The videos were processed, by binarizing, where they are broken down into images that consist only of two tones; black and white.

In binarization it is important to choose the threshold, which is the decision point to make the tone of the image black or white after a certain value. With the application of the threshold it was also possible to eliminate the noise of the image (brightness and shadows), so that only the brightest parts can be observed (Rodríguez-Montaña & Roa-Guerrero, 2017), in this case, hydrogel microspheres. The binarization is expressed with algorithm of Figure

3a. From the decomposition of each video, a sequence of 18,000 binarized frames was obtained, by which the centroids of the particles were obtained for each frame expressed in pixel coordinates. In addition, a data table of the coordinates of each centroid for each image was generated. The centroid were calculated with equations 1 and 2 (Myler & Weeks, 1993).

$$X_c = \frac{1}{A} \sum_{i=1}^N X \quad (1)$$

$$Y_c = \frac{1}{A} \sum_{i=1}^M Y \quad (2)$$

where  $X_c$  and  $Y_c$  are the centroids coordinates,  $X$  and  $Y$  are the coordinates of the  $i$ -th pixel of the object and  $A$  is the object area,  $N$  are the pixels of the width of the image and  $M$  represents the pixels at the top of the image (Myler & Weeks, 1993).

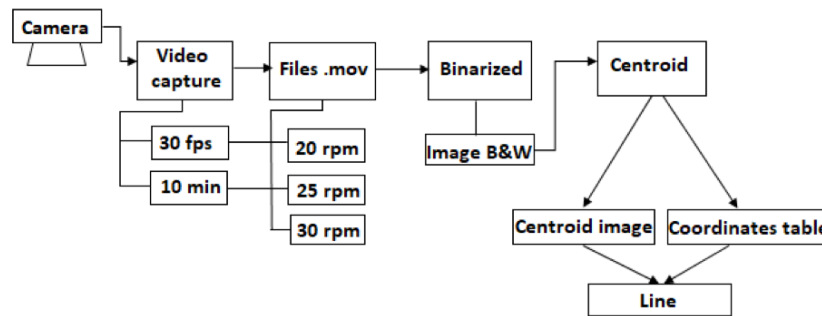


Fig. 2. Proposed methodology diagram for the generation of trajectories.

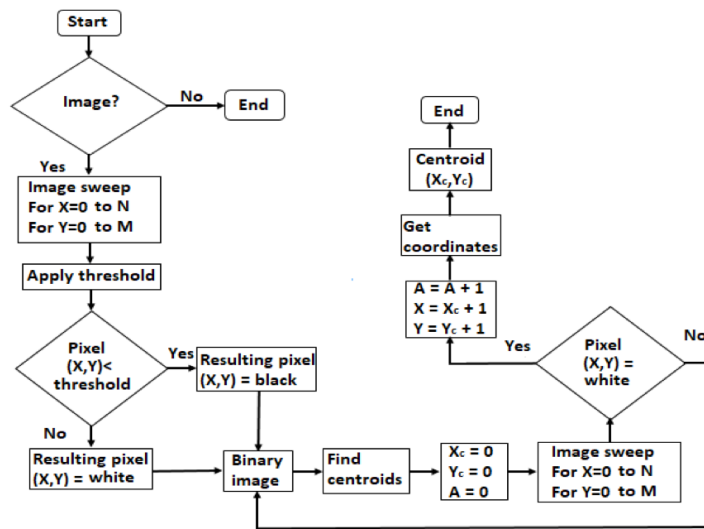


Fig. 3. Flowchart of image binarization and centroid obtaining.

In programming language, the centroids are represented by the algorithm 2 (Figure 3b). Once the coordinates and centroids were obtained, an algorithm to calculate the euclidian distance was applied, which corresponds to Eq. 3.

$$d(i, i - 1) = \sqrt{(X_{ci} - X_{ci-1})^2 + (Y_{ci} - Y_{ci-1})^2} \quad (3)$$

$d(i, i - 1)$  is the distance between two points,  $X_{ci}$  indicates the position of the centroid in  $i$ -th pixel on the  $x$ -axis and  $X_{ci-1}$  is the centroid positions before the  $i$ -th pixel on the  $x$ -axis.  $Y_{ci}$  is the centroid positions in  $i$ -th pixel on the  $y$ -axis,  $Y_{ci-1}$  indicates the position of the centroid before the  $i$ -th pixel on the  $y$ -axis. To determine the distance in two dimensions.

From the centroids and the Euclidean distance, the lines indicating the change of position of each particle were drawn, what are the trajectories within the biorreactor. This was done by comparing each binarized frame and the coordinates found for it, comparing each image with the previous one in order to draw the line that indicates the change of position.

To determine the similarity of the trajectories generated within the fluid, a comparison of the coordinates of the centroids was made frame by frame, of the three videos generated, for each speed of agitation. Through Hamming distance, which is the minimum distance that is accepted to correct an error ( $D_m$ ) and is given by equation (4).

$$D_m = 2x + 1 \quad (4)$$

where  $x$  are the data lines. The minimum distance has a value of 3 (Cisneros Rosero & Sepúlveda Núñez, 2012).

If when comparing the coordinates of the centroids, in each frame,  $D_m \leq 3$ , it can be said that the trajectories generated by the fluid in motion are equal. The Raceway pond was divided into eight sections, where velocity was calculated in seven of them (Figure 1A), this was done by means of equation (5) (Ronald, 1991).

$$\frac{dx}{dt} = kv \quad (5)$$

where  $dx$  is the position change,  $dt$  is the time change,  $k$  is a conversion factor from pixels to meters and  $v$  is the flow velocity represented by the particle velocity (Ronald, 1991).

### 2.3 Experimental determination of hydrodynamics parameter

The hydrodynamic parameters were calculated from the velocity: Reynolds number, Froude number, Power consumption, Power number, Flow, Flow number and hydraulic efficiency, which are presented in the equations 6-12.

$$N_{Re} = \frac{\rho v d_h}{\nu} \quad (6)$$

$$N_{Fr} = \frac{v}{\sqrt{g y_h}} \quad (7)$$

$$P = 2\pi \cdot \frac{\omega}{60} \cdot T \quad (8)$$

$$N_P = \frac{P}{\rho N^3 D_a^5} \quad (9)$$

$$E_P = \frac{N_Q^3 \left[ \frac{D_a}{D} \right]^4}{N_P} \quad (10)$$

where  $Re$  depends on the hydraulic diameter of the channel Eq. (13).  $Fr$  depends of cross section Eq. (14) and power consumption depends on the torque Eq. (15).

$$d_h = \frac{4wh}{2h + w} \quad (11)$$

$$y_h = \frac{h}{2} \quad (12)$$

$$T = \frac{D_a}{2} \cdot m \quad (13)$$

### 2.4 Dead zones

When the fluid velocity is below to 0.05 m/s, dead zones are found inside the bioreactor (Zeng *et al.*, 2015), however, another autors like (Hadiyanto *et al.*, 2013 and Zhang *et al.*, 2015) consider that areas or volumes where fluid velocity is lower than 0.10 m/s are dead zones and the volume fraction of dead zone are defined by Eq. (16).

$$\%dz = \frac{V_{v<0.1}}{V_t} \cdot 100 \quad (14)$$

where  $\%dz$  represent dead zone volume fraction,  $V_{v<0.1}$  is the fluid volume where velocity is below to 0.10 m/s and  $V_t$  is the working volume of the Raceway pond, which was calculated by the Eq. 17, the working volume depends on the Raceway area and the depth of culture, Eq. 18 (Chisti, 2016).

$$V_t = A_R \cdot h \quad (15)$$

$$A_R = \pi \cdot w^2 + (s \cdot R_w) \quad (16)$$

### 3 Results and discussion

#### 3.1 Obtaining trajectories, velocity profiles, $Re$ and $Fr$

The videos obtained were subjected to a pre-processing to eliminate reflections, shadows and region delimitation, since these factors influence the determination of centroids in binarization. Trajectories were obtained by detecting the centroids of fluorescent particles inside the Raceway pond (Figure 4a) in two dimensions. The Raceway pond in grayscale is shown at the top, where the yellow circle particles are highlighted corresponding to hydrogel microspheres, in the lower part is the binarized frame and the centroids of the particles are enclosed in yellow circles. With the treated images, the videos were generated again at 30 fps, to track the movement of fluorescent particles immersed in the liquid medium.

This procedure was carried out for each and every one of the stirrers, using three angular velocities (20, 25 and 30 rpm) for each stirrer. Figs. (4b-6) show the centroids and trajectories generated for each stirrer and each angular velocity, with application of Hamming's minimum distance ( $D_m \leq 3$ ) for coordinate comparison, it was determined that the flow streams that follow the particles, are the same.

The velocity of the particles was taken as the velocity of the liquid medium within the Raceway bioreactor, since when solid tracers are used, the velocity that the particle carries represents the liquid medium velocity as indicated (Martínez González, 2014), in his work he determines the velocity in a part of a glass container with in a sequence of 40 frames. In the present work, the velocity in the complete bioreactor is determined and with a sequence of 18,000 frames, which increases the precision in the measurement. The values of velocity,  $Re$  and  $Fr$  numbers found for each type of agitator are reported in tables (4) - (6).

Figure 4b shows the distribution of the hydrogel microspheres within the liquid phase, where the preferential routes that travel the particles inside the Raceway pond channels are observed, due to the flow generated by the turbine stirrer. When the mixing speed was 20 rpm (Figure 4b), uniform mixing was not achieved and dead zones predominate. As the velocity of agitation increases, the distribution tends to be uniform. When 30 rpm was applied, the microspheres were dispersed over the majority of the Raceway. There is a section of pond, after the exit of the agitator that is in turbulence with a  $Re = 68,959$  (Table 2.), followed by a small dead zone, this is due to the thrust of the agitator into the liquid medium. Since the greatest turbulence is located in the discharge or exit area of the agitator and the current produced tends to be directed towards the central barrier of the Raceway and then distributed throughout the channel. In addition under this conditions  $Fr = 1.11$  was obtained, which indicates that the fluid is normal since it is sought that the values in the Froude number tend to the unit.

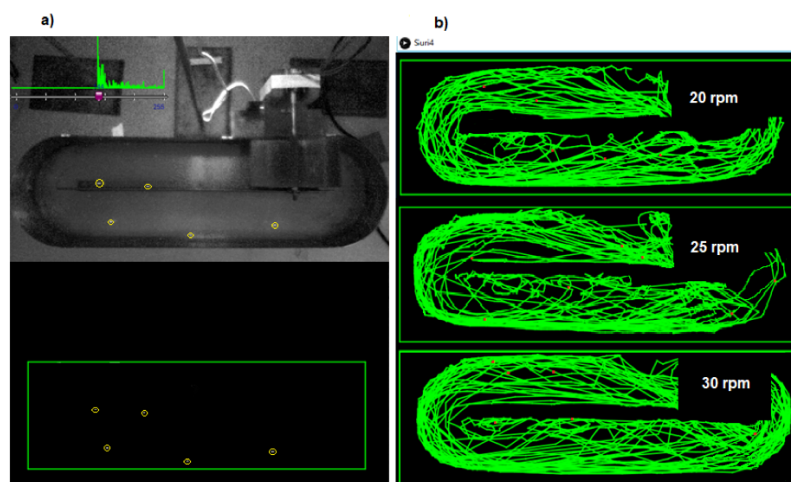


Fig. 4. a). Visualization of fluorescent and centroid particles. b) Trajectories generated with the Turbine stirrer at 20, 25 and 30 rpm.

Table 2. Values of  $\nu$ ,  $Re$  and  $Fr$  in different areas of the Raceway tank, with turbine stirrer.

rpm	20			25			30			
	Zone	$\nu$ (m/s)	$Re$	$Fr$	$\nu$ (m/s)	$Re$	$Fr$	$\nu$ (m/s)	$Re$	$Fr$
a		0.16	19,553	0.32	0.33	41,741	0.68	0.4	50,045	0.81
b		0.08	9,768	0.16	0.09	10,644	0.17	0.3	37,880	0.61
c		0.12	14,583	0.24	0.07	8,141	0.13	0.55	68,959	1.11
d		0.23	28,198	0.46	0.32	39,706	0.64	0.4	50,419	0.81
e		0.13	16,491	0.27	0.31	38,226	0.62	0.21	25,973	0.42
f		0.08	9,575	0.15	0.15	18,597	0.3	0.19	23,169	0.37
g		0.1	12,864	0.21	0.11	13,305	0.21	0.39	48,839	0.79

The value of Reynolds obtained is more than twice that reported by (Crowe *et al.*, 2012), in a pilot Raceway, where for a fluid velocity of 0.25 m/s a  $Re = 26,906$  was obtained. This report shows that the flow is less turbulent, this behavior is also due to the geometric differences of the Raceway ponds used in each job.

When the double paddle stirrer was applied, the existence of dead zones was observed at the beginning of the first curve corresponding to the c zone, on the wall of the pond as well as on the inside of the curve near the central barrier (Figure 5a). With the increase in stirring speed there was an increase in dead zones near central wall, accompanied by increased turbulence in the second straight zone, which corresponds to sections d, e and f. But there was a decrease of dead zones in the second curve that corresponds to section g.

The velocities of the liquid medium produced  $Re$  values above 8,000, ensuring that most of the system is in turbulence (Chisti, 2016), being 6,393 the lowest value of  $Re$  at 20 rpm, upstream of the first curve. Even

with these values, the flow is closer to the turbulence compared to that presented by (Huesemann *et al.*, 2017) which is 7,770 in columns used to simulate open ponds culture conditions, with magnetic stirring systems at 150 rpm.

The values of  $Fr$  reached show that the fluid is in a subcritical state, being  $Fr = 0.74$  the maximum value (Table 3), which indicates that the flow is slow (Mott, 2006). Since in addition to the turbulence a critical or supercritical flow is expected.

The mesh type stirrer produces a distribution of the fluid throughout the tank (Figure 5b), however the fluid currents generated due to the thrust of the paddle are very weak, making a slow flow.  $Re$  values of less than 2,000 are characteristic of a laminar flow (Giles *et al.*, 2003), which does not occur with the mesh type stirrer, even though it is the agitator that produces the lowest  $Re$  values, where the minimum velocity of 0.04 m/s (25 rpm) favors the appearance of dead zones, that arise at velocities lower than 0.10 m/s (Jianke *et al.*, 2015).

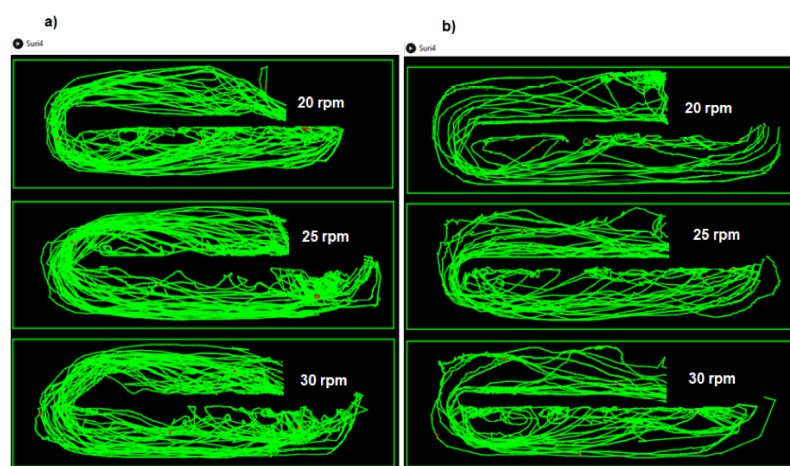


Fig. 5. a) Trajectories generated with the double blade stirrer at 20, 25 and 30 rpm. b) Trajectories generated with the mesh stirrer at 20, 25 and 30 rpm.

Table 3. Values of  $\nu$ ,  $Re$  and  $Fr$  in different areas of the Raceway tank, with double blade stirrer.

rpm	20			25			30			
	Zone	$\nu$ (m/s)	$Re$	$Fr$	$\nu$ (m/s)	$Re$	$Fr$	$\nu$ (m/s)	$Re$	$Fr$
a	0.1	12,138	0.2	0.16	19,869	0.32	0.17	21,234	0.34	
b	0.09	11,204	0.18	0.11	14,351	0.23	0.16	20,100	0.32	
c	0.11	13,920	0.22	0.21	26,143	0.42	0.24	30,033	0.49	
d	0.05	6,393	0.1	0.1	13,081	0.21	0.37	45,936	0.74	
e	0.16	20,023	0.32	0.08	10,200	0.16	0.09	11,721	0.19	
f	0.13	15,711	0.25	0.16	20,303	0.34	0.08	9,718	0.16	
g	0.11	13,871	0.22	0.28	35,106	0.57	0.11	13,279	0.21	

This stirrer generates a maximum velocity of 0.27 m/s (30 rpm) with  $Fr$  number less than 0.54 and minimum  $Re$  number of 4,884, corresponding to transition state. This implies that the microorganisms that are exposed to this stirrer would be in suspension but without reaching an agitation that generates the necessary turbulence so that there is a complete mixing. Since in most sections of the Raceway pond the velocity is below 0.20 m/s (Table 4), in this type of bioreactors a velocity in the liquid medium between 0.20 to 0.60 m/s is needed (Belay, 2002).

The liquid medium distribution and the trajectories of the currents generated by the anchor stirrer can be seen in Figure 6a, when like the turbine stirrer, there is a decrease in dead zones in relation to the increase in angular velocity. There are linear flow patterns in the first straight bioreactor zone. Once the fluid passes the first curve, the predominant flow patterns are the annular, which indicates the presence of eddies near the central barrier. The presence of a dead zone in the first straight zone of the pond persists, near the wall, this is because in addition to having

a discharge area, the paddle also generates suction at output, which causes the liquid to return and flow through the internal part of the channel, sticking to the central barrier.

The maximum velocity found is reported in the d zone, which corresponds to the output of the curve for the three stirring velocities (20, 25 & 30 rpm) that are 0.40 m/s, 0.39 m/s & 0.57 m/s, respectively and the minimum velocity was 0.04m/s at 30 rpm (Table 5). With this stirrer most regions are turbulent in the channel, with Reynolds values above 10,000, except b zone at 20 rpm and e zone at 30 rpm which have the lowest values of  $Re$ , with 8,536 and 4,659 respectively. However, all  $Fr$  values are below unity, which indicates that the flow, is turbulent but slow. In this study, the flow presented is expected to be critical turbulent or turbulent supercritical.

Also the flow produced by the conventional agitator of eight flat blades was studied, since (Chisti, 2016) states that this stirrer is the one that has greater efficiency in terms of mixing in Raceway bioreactors (Figure 6b).

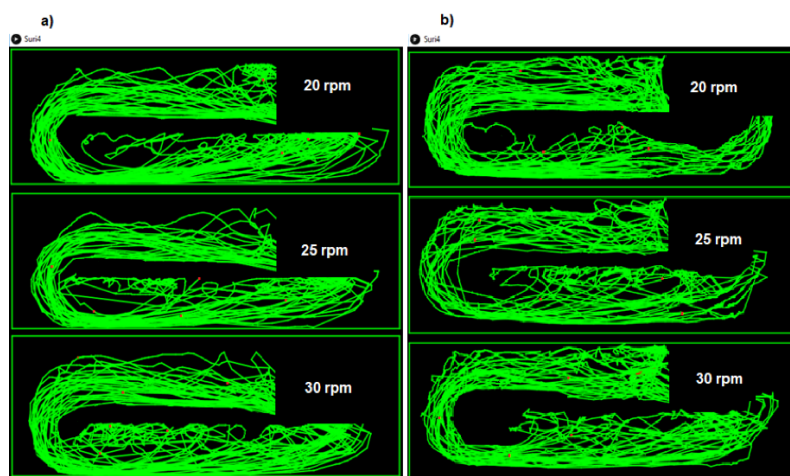


Fig. 6. a) Trajectories generated with the anchor stirrer at 20, 25 and 30 rpm and b) Trajectories generated with the conventional paddlewheel at 20, 25 and 30 rpm.



Table 4. Values of  $\nu$ ,  $Re$  and  $Fr$  in different areas of the Raceway tank, with mesh stirrer.

rpm	20			25			30			
	Zone	$\nu$ (m/s)	$Re$	$Fr$	$\nu$ (m/s)	$Re$	$Fr$	$\nu$ (m/s)	$Re$	$Fr$
a	0.05	6,758	0.11	0.04	4,846	0.08	0.04	5,229	0.08	
b	0.1	12,529	0.2	0.07	8,836	0.14	0.07	9,268	0.15	
c	0.21	26,583	0.43	0.15	18,961	0.31	0.21	26,765	0.43	
d	0.04	4,884	0.08	0.07	9,221	0.15	0.26	32,834	0.53	
e	0.12	15,576	0.25	0.1	11,904	0.19	0.22	26,955	0.44	
f	0.07	9,248	0.15	0.1	13,071	0.21	0.18	22,131	0.36	
g	0.13	16,806	0.27	0.08	10,138	0.16	0.08	10,138	0.16	

For this stirrer it was found a distribution of the fluid is greater when the agitation velocity is 20 rpm, as well as the increase in turbulent areas and velocities higher than 0.2 m/s from 25 rpm, with maximum velocity of 0.46 m/s, that generates  $Re = 57,744$  and  $Fr = 0.93$  (Table 6), corresponding to *e* zone, which indicates that the central part of the channel experiences the greatest turbulence. Figure 6b shows that with the increase in angular velocity the extension of a dead zone in the bioreactor increases that appears upstream of the first curve. The flow is turbulent since most of the values of  $Re$  are above 10,000 (Giles *et al.*, 2003), but the low  $Fr$  values are characteristic of a subcritical flow. Furthermore, the current generated by the stirrer is not sufficient to distribute the particles in the liquid medium throughout the Raceway pond (Ali *et al.*, 2015).

### 3.2 Determination of $P$ , $N_P$ , $Q$ , $N_Q$ , $E_P$

The remaining parameters ( $P$ ,  $N_P$ ,  $Q$ ,  $N_Q$ ,  $E_P$ ) are determined using the average velocity of the Raceway pond, Table 6. Where the hydrodynamic parameters of

each stirrer are presented, for the three stirring speeds. Being the hydraulic efficiency ( $E_P$ ) the main factor for the comparison of the stirrers, since it relates the amount of flow that passes through the stirrer with the power consumed (Uribe Ramírez *et al.*, 2012).

When the stirring speed was 20 rpm (Table 7), the agitator that showed the highest hydraulic efficiency was the anchor and its power consumption was less than that of flat blades, which indicates that with lower power is able to generate a higher volumetric flow. The one with the lowest power consumption was the mesh stirrer and the obtained volumetric flow was the same as that of double blades, but with half of power consumption of this last stirrer. The turbine stirrer presented similar parameters to the classic paddle wheel of flat blades, being the ones that consume more power, but also generate a higher volumetric flow, although its efficiency is below the anchor-type paddle stirrer. However, a complete mixing is not experienced with this stirring speed, since the velocities of the liquid medium at 20 rpm are in the range of 0.08 m/s to 0.14 m/s.

Table 5. Values of  $\nu$ ,  $Re$  and  $Fr$  in different areas of the Raceway tank, with anchor stirrer.

rpm	20			25			30			
	Zone	$\nu$ (m/s)	$Re$	$Fr$	$\nu$ (m/s)	$Re$	$Fr$	$\nu$ (m/s)	$Re$	$Fr$
a	0.09	11,204	0.18	0.13	16,481	0.27	0.09	10,874	0.18	
b	0.07	8,536	0.14	0.09	11,311	0.18	0.12	15,398	0.25	
c	0.17	21,074	0.34	0.16	20,371	0.33	0.14	17,974	0.29	
d	0.4	50,543	0.82	0.39	48,951	0.79	0.57	68,361	1.1	
e	0.33	41,315	0.67	0.21	26,427	0.43	0.04	4,659	0.08	
f	0.13	16,226	0.26	0.14	17,014	0.27	0.17	21,041	0.34	
g	0.12	14,524	0.23	0.11	13,215	0.21	0.24	29,390	0.47	

Table 6. Values of  $\nu$ ,  $Re$  and  $Fr$  in different areas of the Raceway tank, with conventional paddlewheel.

rpm	20			25			30			
	Zone	$\nu$ (m/s)	$Re$	$Fr$	$\nu$ (m/s)	$Re$	$Fr$	$\nu$ (m/s)	$Re$	$Fr$
a	0.2	25,274	0.41	0.21	26,363	0.43	0.13	16,559	0.27	
b	0.07	9,025	0.15	0.13	15,753	0.25	0.11	14,039	0.23	
c	0.16	20,348	0.33	0.2	25,113	0.41	0.31	38,176	0.62	
d	0.17	20,688	0.33	0.43	54,270	0.88	0.3	37,996	0.61	
e	0.1	12,968	0.21	0.18	22,728	0.37	0.46	57,744	0.93	
f	0.12	14,984	0.24	0.24	29,746	0.48	0.37	46,684	0.75	
g	0.15	18,206	0.29	0.23	28,859	0.47	0.21	25,894	0.42	

In the work of Sompech *et al.* (2012) three agitation speeds are used (30, 35 and 45 rpm) with which velocities are obtained in the fluid of 0.12, 0.14 & 0.19 m/s respectively, in the Raceway pond simulation of 5,000 m<sup>2</sup>. In this work, the maximum angular speed used was 30 rpm, with which flow velocities were obtained from 0.13 to 0.31 m/s.

The linear velocity is directly affected by the angular velocity, therefore an increase in the rpm increases the linear velocity of the fluid (Jianke *et al.*, 2015), and this is reported in Table 6. Where it is observed in increase of the speed produced by the stirrers, highlights the increase with the flat blades paddlewheel, which is reported of 0.20 m/s, at 25 rpm this agitator was the one that had the highest performance with an efficiency of 0.0146. However, this velocity is below that recommended by Huesemann *et al.* (2017) in which they use an average speed in the channel of 0.28 m/s.

Jianke *et al.* (2015) exposes that a Raceway pond of 1.4 m long and 0.4 m wide channel, consume around 392.5 W that were measured, with a paddlewheel at 20 rpm, versus 19.1 W theoretically calculated. On the other hand, Li *et al.* (2014) studied three agitators of four modified pallets in the lower part of each paddle (zigzagged, curved forward and curved back) and compare them to the flat paddle in a Raceway pond 1 m wide and 2.4 m long. In their study, they report a minimum consumption of 0.78 W and a maximum of 7.40 W, in a range of angular speed of 7-16 rpm, and flow rate between 0.15-0.33 m/s. In the work they do (Zeng *et al.*, 2015), a paddlewheel is used at different degrees of inclination (5, 10 & 15°) in CFD simulation and it is compared to the traditional paddlewheel. In this study they obtain velocity profiles between 0.27-0.28 m/s and power consumption from 11.5- 12.8 W in a Raceway pond 4.5 m long and 1.9 m width.

The highest consumption value reported here is 0.58 W at 20 rpm, 0.72 W at 25 rpm and 0.84 W at 30 rpm and velocities of 0.12, 0.14 y 0.31 m/s (Table 7), with turbine stirrer in the Raceway pond of 0.70 m long and 0.20 m wide. The agitator that requires less power is the mesh with maximum values of 0.41 W, the difference in the values falls on the weight of each stirrer, while lighter, it will be easier to move.

The mixing of the liquid medium contained in the channels of the Raceway pond was favoured with the stirring speed of 30 rpm, where the liquid stirred by the turbine reached a velocity of 0.31 m/s (Table 7), which is greater than the velocity presented by (Liffman *et al.*, 2013), that in a Raceway bioreactor simulation study has a velocity of 0.30 m/s using a paddlewheel.

The power consumption of the turbine stirrer had an increase that is justified with the hydraulic efficiency obtained that was 0.0439, which represents a ratio of 3.14 with respect to the efficiency of the flat paddle stirrer, which barely reached a velocity of 0.21 m/s. This means that, the turbine stirrer at 30 rpm is three times more efficient than the flat paddle stirrer and thanks to the velocity generated, it is able to maintain turbulence throughout the bioreactor, causing a greater fluid distribution (Figure 4b).

In Table 6, the flow values contained in the Raceway pond show that, at 30 rpm, turbine stirrer generates a greater volumetric flow that is 0.0016 m<sup>3</sup>/s, followed by the flat paddle stirrer with  $Q = 0.0011$  m<sup>3</sup>/s. At 25 rpm the stirrers that produced the highest flow rate were the flat paddles with  $Q = 0.001$  m<sup>3</sup>/s, followed by the turbine and anchor agitator that had the same value of 0.0007 m<sup>3</sup>/s. And at 20 rpm, the anchor stirrer produced a flow of 0.0007 m<sup>3</sup>/s and the turbine had the same flow value as the flat bladed one, with  $Q = 0.0006$  m<sup>3</sup>/s. The flow rate in Raceway bioreactors was studied by (Liffman *et al.*, 2013), in which they report that  $Q = 0.248$  m<sup>3</sup>/s at velocity of 0.30 m/s, this value is much higher than

those presented in this study, however, it is attributed to the differences in the geometric magnitudes used in the Raceway channels, since (Liffman *et al.*, 2013) use a 5 m channel width in a CFD simulation in comparison of the channel width of 0.1 m, which is the one used in this work and it should also be noted that the data obtained are experimental values.

### 3.3 Dead zones

The raceway bioreactor has an area of 1314.16 cm<sup>2</sup>, which corresponds to a work volume of 6.57 l that was calculated with Eq. 17. To determine the percentage of volume corresponding to the dead zones (%dz) the volume of the areas, where there is no trajectory presence of the hydrogel microspheres was calculated. The data obtained are reported in the Table 7. With all the agitators the highest %dz is reported when the agitation speed is 20 rpm, where the mesh stirrer has a 31.30% of dead zones and the flat blade stirrer shows the best distribution at this agitation speed, presented 12.80% of dead zones. This difference is due to the fact that the mesh stirrer has less contact surface with the water and also has two less paddles than the flat paddle stirrer. In all cases the mesh stirrer has the highest number of dead zones. It is expected that as the speed of the liquid medium increases the %dz

decreases (Hadiyanto *et al.*, 2013). However, this was only observed in two agitators. With the double blade, at 20 rpm presented 22.65%, at 25 rpm decreased to 14.70% and at 30 rpm the decrease in dead zones was not evident.

On the other hand, with turbine stirrer, the dead zones decreased from 15.38% (20 rpm) to 12.75% (25 rpm) and the lowest value of %dz = 8.52 at 30 rpm was obtained. Hadiyanto *et al.* (2013) obtained reduction of dead zones in Raceway bioreactors with different aspect ratios, reporting a maximum %dz of 18 and a minimum of 3% approximately.

Some agitators exhibit undesirable behavior in terms of decreasing dead zones, as the case of the anchor type stirrer, that at 20 rpm presents a %dz = 20.82 and by increasing the agitation speed to 25 rpm it also increases the %dz, but when the agitation speed is 30 rpm the dead zones decrease by almost 10%. The mesh and flat blade stirrers decrease their %dz at 25 rpm, but when the agitation increases to 30 rpm, dead zones also increase.

Sompech *et al.* (2012) studied the diminution of dead zones by adding baffles in the curves of a Raceway, when they applied a single baffle, at 30 rpm, the %dz was 6.7, with conventional paddlewheel, which is 1.82% less than that found in this study with the turbine stirrer.

Table 7. Hydrodynamic parameters at different agitation speeds and dead zones in % of volume.

Stirres (30 rpm)	$v$ (m/s)	$P$ (W)	$Q$ (m <sup>3</sup> /s)	$N_P$	$N_Q$	$E_P$	%dz
<b>Double blade</b>	0.14	0.75	0.0007	3148	3.26	0.0045	14.63
<b>Mesh</b>	0.13	0.41	0.0007	1712	3.09	0.007	24.69
<b>Anchor</b>	0.19	0.81	0.0009	3449	4.41	0.0102	13.79
<b>Turbine</b>	0.31	0.86	0.0016	3646	7.31	0.0439	8.52
<b>Paddlewheel</b>	0.31	0.84	0.0011	3525	4.94	0.014	14.26
Stirres (25 rpm)	$v$ (m/s)	$P$ (W)	$Q$ (m <sup>3</sup> /s)	$N_P$	$N_Q$	$E_P$	%dz
<b>Double blade</b>	0.12	0.62	0.0006	2624	2.7	0.0031	14.7
<b>Mesh</b>	0.08	0.34	0.0004	1427	1.89	0.0019	19.35
<b>Anchor</b>	0.15	0.68	0.0007	2874	3.46	0.0059	23.27
<b>Turbine</b>	0.14	0.72	0.0007	3038	3.23	0.0045	12.75
<b>Paddlewheel</b>	0.2	0.7	0.001	2938	4.71	0.0146	12.21
Stirres (20 rpm)	$v$ (m/s)	$P$ (W)	$Q$ (m <sup>3</sup> /s)	$N_P$	$N_Q$	$E_P$	%dz
<b>Double blade</b>	0.08	0.5	0.0004	4100	2.35	0.0013	22.65
<b>Mesh</b>	0.08	0.27	0.0004	2230	2.2	0.002	31.3
<b>Anchor</b>	0.14	0.55	0.0007	4490	4	0.0059	20.82
<b>Turbine</b>	0.12	0.58	0.0006	4747	3.37	0.0033	15.38
<b>Paddlewheel</b>	0.12	0.56	0.0006	4590	3.58	0.0041	12.8

Another case study of dead zones is what they do (Zhang *et al.*, 2015), where they add baffles at the bottom of a Raceway pond as well as curves and report a maximum value of 2.84% of dead zones. Although significant decreases in dead zones are reported, there is no experimental evidence to corroborate this, unlike the present study where dead zones were determined experimentally.

## Conclusions

Through a variant of the velocimetry method by particle tracking, the trajectories were determined, velocity profiles,  $Re$ ,  $Fr$ ,  $P$ ,  $N_P$ ,  $Q$ ,  $N_Q$ ,  $E_P$ , using fluorescent particles immersed in the liquid medium, used as solid tracers. The comparison of the five stirrers allowed observing with which of them there is a better distribution of the fluid, decreasing dead zones due to the presence of turbulence.

When stirring speeds of 20 and 25 rpm were applied the stirrers that presented greater efficiency were the anchor and the flat paddle respectively, but the velocities reached were low, causing most of the bioreactor to be in a transition regime.

When it was stirred at 30 rpm with the turbine it was reached at a velocity higher than 0.30 m/s, which generates intense currents in low viscosity fluids, these currents extend throughout the pond and break the stagnant liquid masses, with this Reynolds values are obtained from 23,000 to 68,000, so turbulence is assured throughout the channel and %dz was the minimum. The  $Fr$  number indicates that the flow current is near a critical or normal flow. In addition, the increase in angular velocity causes an increase in the flow rate generated by the stirrers.

A higher linear velocity is presented with the turbine than with the classic paddlewheel at the same angular velocity. This is due to the geometric configuration of turbine stirrer, where the dimensions and radius of the curves of the paddle allow it to enter the liquid more easily, decreasing the energy expended to rid the surface tension of the water and the shear stress in the fluid, this is reflected in a decrease in the power consumption required by the paddle to generate a greater volumetric flow. These hydrodynamic conditions are also achieved thanks to the aspect ratio (channel width/depth = 2) maintained by the Raceway pond and the geometric relationships involved between the stirrer and the channel. The flat paddle stirrer needs more energy to reach the velocity

and Reynolds number values obtained with the curved blade turbine stirrer. So the geometric configuration of the agitator that exposes the present study, has a better performance and produces a complete mix within the Raceway pond channels and a lower power consumption than conventional paddlewheel.

## Acknowledgements

The first author thanks the support to Consejo Nacional de Ciencia y Tecnología (CONACYT) for the scholarship granted to study the master's degree in biotechnology within the postgraduate program of Universidad Politécnica de Pachuca, included in the Padrón Nacional de Postgrados de Calidad.

## Abbreviations

%dz	Dead zone volume fraction
A	Object area (pixels <sup>2</sup> )
$A_R$	Raceway area
$d(i, i - 1)$	Distance between two point
D	Chanel diameter (m)
$D_a$	Stirrer diameter (m)
$D_m$	Hamming's distance minimal
dh	Hydraulic diameter (m)
dx	Position change (pixels)
dt	Time change (s)
$E_P$	Hydraulic efficiency of stirrer
h	Depth of culture
k	Conversion factor (pixels to meters)
M	Total number of pixels in image height
m	Stirrer mass (Kg)
N	Total number of pixels in image width
$N_{Re}$	Reynolds number
$N_{Fr}$	Froude number
$N_P$	Power number
$N_Q$	Flow number
P	Power (Watts)
Q	Flow (m <sup>3</sup> /s)
$R_w$	Raceway width
s	Raceway straight zone
T	Torque (Kgf-cm)
v	Velocity (liquid and particle) (m/s)
$V_{v<0.10}$	Fluid volume when velocity is lower than 0.10 m/s
$V_t$	Working volume
w	Channel width
x	Data lines

$X$	Object $i$ -th pixel coordinates on the $x$ -axis
$X_c$	Centroid coordinate on the $x$ -axis
$X_{ci}$	Centroid coordinate in $i$ -th pixel on the $x$ -axis
$X_{ci-1}$	Centroid coordinate before $i$ -th pixel on the $x$ -axis
$Y$	Object $i$ -th pixel coordinates on the $y$ -axis
$Y_c$	Centroid coordinate on the $y$ -axis
$Y_{ci}$	Centroid coordinate in $i$ -th pixel on the $y$ -axis
$Y_{ci-1}$	Centroid coordinate before $i$ -th pixel on the $y$ -axis
$y_h$	Channel cross section
<i>Greek symbols</i>	
$g$	Gravity acceleration ( $m/s^2$ )
$\rho$	Water density ( $kg/m^3$ )
$\pi$	Conversion factor pi
$\nu$	Water viscosity Pa-s (cp)
$\omega$	Angular velocity, revolutions per minute (rpm)

## References

- Ali, H., Taqi A., C., Ho-Sung, Y., Younghae, D., & Cheol W., P. (2015). Numerical prediction of algae cell mixing feature in raceway ponds using particle tracing methods. *Biotechnology and Bioengineering* 112, 297-307.
- Ayala Gómez, R., Domínguez Murillo, E., & Quintero Toscano, A. (1996). *Elementos de la Topología General*. Madrid: Addison-Wesley Iberoamericana-España.
- Belay, A. (2002). Mass culture of spirulina outdoors –the earthrise farms experience. In: *Spirulina platensis (Arthrospira): Physiology, Cell-Biology and Biotechnology*. (A. Vonshak ed.), Pp. 131-158. Taylor & Francis, Israel.
- Borowitzka, M. A. (2005). Culturing microalgae in outdoor ponds. In: *Algal Culturing Techniques* (R. A. Andersen ed.), Pp. 205-218. Elsevier, China.
- Cisneros Rosero, A. H., & Sepúlveda Núñez, D. (2012). *Código de Hamming para detección y corrección de errores*. Tesis de Maestría en Ciencias de la Información y Comunicaciones, Bogotá.
- Chisti, Y. (2013). Raceways-based production of algal crude oil. In: *Microalgal Biotechnology: Potential and Production*. (C. Posten y C. Walter eds.), Pp. 195-216. De Gruyter. Alemania.
- Chisti, Y. (2016). Large-scale production of algal biomass: Raceway ponds. In *Algae Biotechnology*, Bux F., Chisti Y. (eds), Pp. 21-40. Springer, Cham.
- Contreras Flores, C., Peña Castro, J. M., Flores Cotera, L. B., & Cañizares Villanueva, R. O. (2003). Avance en el diseño conceptual de fotobiorreactores para el cultivo de microalgas. *Interciencia* 28, 450-456.
- Crowe, B., Attalah, S., Agrawal, S., Waller, P., Ryan, R., Van Wagenen, J., *ldots* Huesemann, M. (2012). A comparison of nanochloropsis salina growth performance in two outdoor pond designs: Conventional raceways versus the ARID pond with superior temperature management. *International Journal of Chemical Engineering* 2012, Article ID 920608.
- Geankoplis, C. J. (2003). Principles of momentum transfer and applications. In: *Transport Processes and Separation Process Principles*. (C. J. Geankoplis ed.), Pp. 121-234. Prentice Hall, México.
- Giles, R. V., Evett, J. B., & Liu, C. (2003). Flow in Open Channels. In: *Fluid Mechanics and Hydraulics*. 3 ed. (M. J. Norte Ed.), Pp. 193-234. McGraw-Hill, España.
- Hadiyanto, H., Elmore, S., Van Gerven, T., & Stankiewicz, A. (2013). Hydrodynamic evaluation in high rate algae pond (HRAP) design. *Chemical Engineering* 217, 231-239.
- Hazlebeck, D. A. (2011). Microalgae Growth Pond Design. Patent Application Publication, Pub. No.: US 2011/0287531 A1 (24). El Cajón CA.
- Hernández Pérez, A., & Labbé, J. I. (2014). Microalgas, cultivo y beneficios. *Revista de Biología Marina y Oceanografía* 49, 157-173.
- Huesemann, M., Dale, T., Crowe, B., Barry, A., Valentine, D., Yoshida, R., ... Cullinan, V. (2017). Simulation of outdoor pond cultures using indoor LED-lighted and temperature-controlled raceway ponds and phenometrics photobioreactors. *Algal Research* 21, 178-190.

- Huesemann, M., Williams, P., Edmunson, S., Chen, P., Cullinan, V., Crowe, B., & Lundquist, T. (2017). The laboratory environmental algae pond simulator (LEAPS). *Algal Research* 26, 39-46.
- Jianke, H., Qu, X., Wan, J., Li, Y., Zhu, F., Wang, J., ... Li, W. (2015). Investigation on the performance of raceway ponds with internal structures by the means of CFD simulations and experiments. *Algal Research* 10, 64-71.
- Kanhaiya, K., Sanjiv k, M., Anupama, S., Min, S. P., & Won Yang, J. (2015). Recent trends in the mass cultivation of algae in raceway ponds. *Renewable and Sustainable Energy Reviews* 51, 875-885.
- Li, Y., Zhang, Q., Wang, Z., Wu, X., & Cong, W. (2014). Evaluation of power consumption of paddle wheel in an open raceway pond. *Bioprocess and Biosystems Engineering* 37, 1325-1336.
- Liffman, K., Paterson, D. A., Liovic, P., & Bandopadhyay, P. (2013). Comparing the energy efficiency of different high rate algal raceway pond designs using computational fluid dynamics. *Chemical Engineering Research and Design* 91, 221-226.
- López Hinojosa, M. (2006). *Un nuevo algoritmo en la técnica de la velocimetría por imágenes de partículas*. Tesis de maestría en Ciencias de la Comunicación, Instituto Politécnico Nacional, México.
- Martínez Gonzáles, A. (2014). *Estudio y caracterización de un sistema de velocimetría óptica para hacer mediciones de temperatura y velocidad*. Tesis Doctoral en Ciencias (óptica), Centro de investigaciones en óptica, León Guanajuato, México.
- Martínez-Palma, N., Martínez-Ayala, A., & Dávila-Ortíz, G. (2015). Determination of antioxidant and chelating activity of protein hydrolysates from spirulina (*Arthrospira maxima*) obtained by simulated gastrointestinal digestion. *Revista Mexicana de Ingeniería Química* 14, 25-34.
- Martínez-Ramírez, J. D., & Gonzáles, F. J. (2006). *Velocímetro de partículas basado en imágenes digitales*. Tesis de maestría en Ciencias Aplicadas, Universidad Autónoma de San Luis Potosí, San Luis Potosí, México.
- McCabe, W. L., Smith, J. C., & Harriot, P. (2005). Fluid flow phenomena. In: *Unit Operations of Chemical Engineering* (J. C. Warren L. McCabe eds.), Pp. 45-67. McGraw-Hill, New York.
- Mendoza Guzmán, H. S., De la Jara Valido, A., & Portillo Hahnefeld, E. (2011). *Planta Piloto de Cultivo de Microalgas* (1ra. ed.). Canarias: Gráficas tenerife.
- Mott, R. L. (2006). Open channel flow. In: *Applied Fluid Mechanics* (R. L. Mott ed.), Pp. 2018-234. Pearson Prentice Hall. Nex Jersey.
- Myler, H. R., & Weeks, A. R. (1993). *The Pocket Handbook of Image Processing Algorithms in C*. New Jersey: Prentice Hall.
- Navarro-Peraza, R. S., Soto-León, S., Contreras-Andrade, I., Piña-Valdez, P., Viveros-García, T., Cuevas-Rodríguez, E. O., & Nieves-Soto, M. (2017). Effects of temperature and nitrogen limitation on growth kinetics, proximate composition and fatty acid profile of *Nannochloropsis* sp. *Revista Mexicana de Ingeniería Química* 16, 359-369.
- Prussi, M., Buffi, M., Casini, D., Chiaramonti, D., Martelli, F., Carvevale, Tredecchi, M. R., Rodolfi, L. (2014). Experimental and numerical investigations of mixing in raceway ponds for algae cultivation. *Biomass and Bioenergy* 67, 390-400.
- Radmann, E. M., Reinehr, C. O., & V. Costa, J. A. (2007). Optimization of the repeated batch cultivation of microalga *Spirulina platensis* in open raceway ponds. *Aquaculture* 265, 118-126.
- Raffo-Durán, J., Figueredo-Cardero, A., & Dustet-Mendoza, J. C. (2014). Características de la hidrodinámica de un biorreactor industrial tipo tanque agitado. *Revista Mexicana de Ingeniería Química* 13, 823-839.
- Richmond, A. (2004). Principles for attaining maximal microalgal productivity in photobioreactors: an overview. *Hydrobiologia* 512, 33-37.
- Robles-Heredia, J. C., Sacramento-Rivero, J. C., Ruiz-Marín, A., Baz-Rodríguez, S., Canedo-López, Y., & Narváez-García, A. (2016). Evaluación del crecimiento celular, remoción de nitrógeno y producción de lípidos por *Chlorella vulgaris* a diferentes condiciones de aireación

- en dos tipos de fotobiorreactores anulares. *Revista Mexicana de Ingeniería Química* 15, 361-377.
- Rodríguez-Montaña, D. F., & Roa-Guerrero, E. E. (2017). Detección de trayectorias de espermatozoides humanos mediante técnicas de procesamiento de video. *Revista Mexicana de Ingeniería Biomédica* 38, 115-125.
- Ronald J., A. (1991). Particle- image techniques for experimental fluid mechanics. *Annual Reviews* 26, 261-304.
- Ronald J., A. (2005). Twenty years of particle image velocimetry. *Experiments in Fluids* 39, 159-169.
- Sanjeev Mishra, M., & Kaustubha. (2015). Growth characteristics of different algal species. In: *Algal Biorefinery: An Integrated Approach*. (D. Das ed.), Pp. 59-72. Springer International Publishing, New Delhi, India.
- Sompech, K., Chisti, Y., & Srinophakun, T. (2012). Design of raceway ponds for producing microalgae. *Future Science*, 387-397.
- Tomaselli, L. (2004). The microalgal cell. In: *Handbook of Microalgal Culture: Biotechnology and Applied Phycology*. (A. Richmond ed.), Pp. 3-19. Blackwell Science. Australia.
- Uribe Ramírez, A. R., Rivera Aguilera, R., Aguilera Alvarado, A. F., & Murrieta Luna, A. (2012). Agitación y mezclado. *Enlace Químico*, 22-30.
- Vonshak, A. (2002). Spirulina: Growth, physiology and biochemistry. In: *Spirulina platensis (Arthrospira) Physiology, Cell-Biology and Biotechnology*, (A. Vonshak ed.), Pp. 43-65. Taylor and Francis. Londres.
- Zeng, F., Huang, J., Meng, C., Zhu, F., Chen, J., & Li, Y. (2015). Investigation on novel raceway pond with inclined paddle wheels through simulation and microalgae culture experiments. *Bioprocess Biosystems Engineering* 39, 169-180.
- Zhang, Q., Xue, S., Yan, C., Wu, X., Wen, S., & Cong, W. (2015). Installation of flow deflectors and wing baffles to reduce dead zone and enhance flashing light effect in an open raceway pond. *Bioresource Technology* 198, 150-156.